DESIGN AND EXPERIMENT OF TRANSVERSE AXIAL FLOW CORN FLEXIBLE THRESHING DEVICE

/

横轴流玉米柔性脱粒元件的设计与试验

Huabiao LI, Qihuan WANG, Jie MA, Yanan WANG, Dong YUE, Duanyang GENG*)
School of Agricultural and Food Engineering, Shandong University of Technology, Zibo, 255000, China
E-mail: dygxt@sdut.edu.cn

DOI: https://doi.org/10.35633/inmateh-69-43

***Keywords**: Corn, grain direct harvest, flexible threshing, broken rate, impurity rate.*

ABSTRACT

In order to solve the problem of high broken rate and impurity rate in the direct harvesting of corn kernels in China, a flexible threshing element with variable stiffness consisting of a conical spring and rasp bar was developed on the basis of the existing horizontal axial-flow corn threshing cylinder structure to achieve low loss harvesting of corn kernels. Through mechanical analysis of the key components of the threshing element, its structure and operating parameters were determined. Then, orthogonal tests were carried out using the feed amount, threshing clearance and cylinder speed as the test factors, and the broken rate and impurity rate of the corn kernels as the test indicators. The results showed that the feed amount, threshing clearance and cylinder speed had a significant effect on the broken rate and impurity rate of corn kernels; the optimum parameters for the corn variable stiffness flexible threshing device were feed amount 6.1 kg·s^{-1}, threshing clearance 40 mm and cylinder speed 392 r·min^{-1}. The broken rate of corn kernels was 1.67% and impurity rate 1.03%. The test results fully met the requirements of the national standards for corn harvesting operations. This study provides a technical basis for the application of the axial flow corn flexible threshing device in the corn direct harvesting combine.

摘要

为了解决我国玉米籽粒直收过程中籽粒破碎率和含杂率高的问题，在现有横轴流玉米脱粒滚筒结构的基础上，研制了一种锥形弹簧和短纹杆组成的变刚度玉米柔性脱粒元件，实现了玉米籽粒的低损收获。通过对脱粒元件关键部件的力学分析，确定了其结构和工作参数。以玉米果穗喂入量、脱粒间隙和滚筒速度为试验因素，以玉米籽粒的破碎率和含杂率作为试验指标，进行了正交试验。结果表明：果穗喂入量、脱粒间隙和滚筒速度对玉米籽粒破碎率与含杂率均有显著影响；玉米变刚度柔性脱粒装置的最佳参数喂入量 6.1kg·s^{-1}，脱粒间隙 40mm，滚筒速度 392r·min^{-1}。此时，玉米籽粒的破碎率为 1.67%，含杂率为 1.03%。试验结果完全符合玉米收获作业的国家标准要求。本研究为轴流玉米柔性脱粒装置在玉米籽粒直收联合收获机中的应用提供了技术依据。

INTRODUCTION

Corn is not only an important food crop in China, but also has important application value in feed, chemical, energy and other fields *(Srison et al., 2016; Yang et al., 2021)*. In recent years, with the large-scale development of corn planting, labor shortage during the corn harvest season has become an increasingly prominent problem. The direct harvest of corn kernels can complete ear picking, threshing, separation and cleaning operations at one time, which greatly shortens the harvest cycle, effectively saves labor costs and solves the problem of labor shortage *(Li et al., 2020; Yang et al., 2021)*. Therefore, direct harvesting of corn kernels is of great significance for shortening the corn harvest cycle, saving production costs, and promoting the mechanization of corn agriculture *(Akubuo, 2002; Bratan et al., 2019; Chai et al., 2020).*

[1] *Huabiao LI, Postgraduate; Qihuan WANG, Postgraduate; Jie MA, Postgraduate; Yanan WANG, Postgraduate; Dong YUE, Postgraduate; Duanyang GENG, Professor.*

Threshing is a key part of the corn direct harvesting, which directly affects the quality and performance of the entire corn harvest *(Yang et al., 2021)*. Broken rate and impurity rate are important indicators to evaluate the quality of threshing operations *(Shahbazi and Shahbazi, 2018; Su et al., 2020)*. Countries represented by Germany, the United States and other countries usually use combine harvesting machines to directly harvest corn. Large-scale corn harvesters developed by well-known agricultural machinery brands such as John Deere, CASE, and CLASS have high efficiency and degree of mechanization *(Fu et al., 2019)*. In China, scientific research institutions and related enterprises, such as Foton Lovol, Wuzheng Group, and Yongmeng Company, have done a lot of research on corn grain combine harvesters, and have had good field test results in various provinces. However, due to the high grain moisture content of corn harvested in my country, there is still serious kernel damage *(Feng et al., 2019, Chen, 2020, Wang, 2021).*

In order to reduce the rate of corn kernel broken, Chinese scholars have carried out a lot of research. In terms of threshing device, *Srison et al.* explored the effects of threshing cylinder structural parameters and corn characteristics on corn threshing damage and power consumption *(Srison et al., 2016)*. Pužauskas and other studies found that the concave plate structure is an important factor affecting the separation rate of grains, as well as the breakage rate and loss rate of grains *(Pužauskas et al., 2017)*. *Xie et al, (2019),* designed a flexible rod-tooth-type threshing cylinder. Compared with rigid rod-tooth, the flexible rod-tooth can greatly reduce the broken rate of grains. However, most of the current research is the experimental study of the threshing process and technical parameters of the threshing device on the damage to the grain, and there is a lack of innovation and research on the threshing element of the large-scale threshing device of the corn kernel harvester.

In order to solve the above problems, on the basis of the characteristics of the existing threshing cylinder, combined with the characteristics of corn in China, a flexible threshing device with variable stiffness was designed. Through multi-factor orthogonal test, the factors affecting the broken rate and impurity rate of grains were analyzed, and the optimal working parameters were determined. It is hoped that this study can solve the problem of high loss rate and impurity rate in the process of direct harvesting of corn kernels, and improve the quality of corn combine harvesters.

MATERIAL AND METHODS

Overall Structure and Working Principle

The whole structure of the corn variable stiffness flexible threshing device is shown in Fig. 1. It mainly consists of threshing cylinder, upper cover, the guide plate, frame, adjusting concave plate, and screw conveyor, feeding port, blanking plate, grain box, motor and other components.

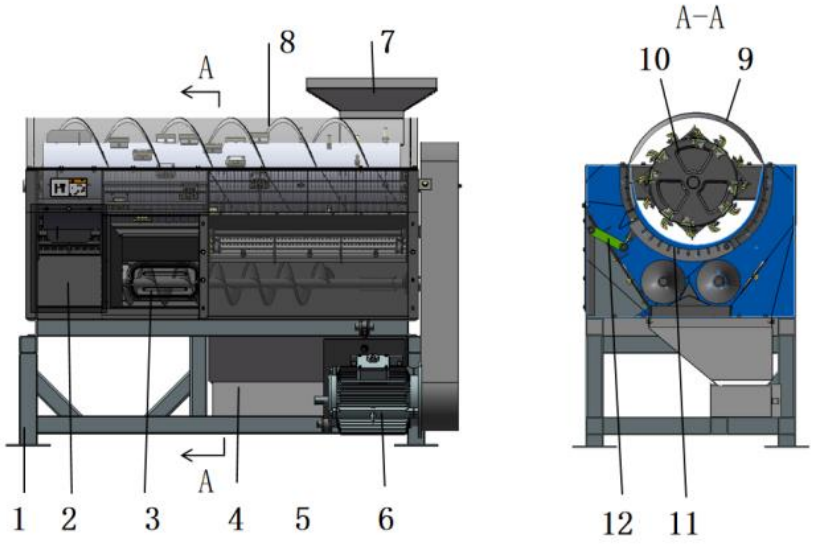

Fig. 1 - Overall structure diagram of flexible threshing device with variable stiffness

1. Frame; 2. Cob outlet; 3. Grain screw conveyor; 4 Grain box; 5. Adjustable concave plate; 6. Electric motor; 7. Corn inlet; 8. Upper cover; 9. The guide plate; 10. Threshing cylinder; 11. Concave; 12. Adjustment device

The corn flexible threshing device adopts the principle of radial feeding and axial flow threshing. When the threshing device is working, the cylinder is driven by the motor, and the corn ears continuously enter the threshing device from the feeding inlet. The ears are forced by the spiral of spike tooth at the front of the cylinder to the threshing section, where they are subjected to the blows of the threshing tooth and striker, the squeezing and friction between the threshing concave plates and the impact between the ears to complete the threshing. Finally, the threshed grains are transported to the grain box through the screw conveyor, and the corncob is discharged from the outlet to complete the whole process.

Design of Threshing Elements

The structure of the threshing element will have a large effect on the kernel broken rate and impurity rate *(Kiniulis et al., 2017; Bratan et al., 2019).* The variable stiffness flexible threshing element designed in this study is shown in Fig. 2. It mainly consists of conical spring seat, cover plate, conical spring, striker block, tension bolt and connecting shaft. The connecting shaft acts on the conical spring seat and the striker block, and the back of the striker block is in contact with the conical spring by the preload of the bolt, and the variable stiffness flexible threshing of the striker block is realized by the variable stiffness characteristic of the conical spring.

The force analysis of the corn cob and threshing element is shown in Fig. 3.

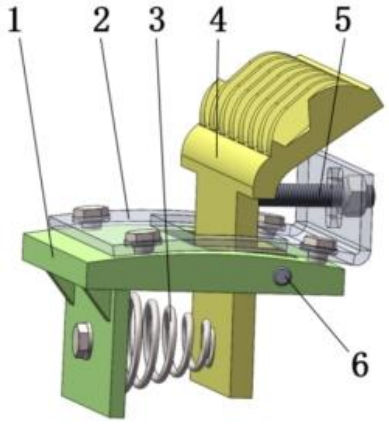

Fig. 2 - The structure of the threshing element
1. Conical spring seat; 2. Cover plate; 3. Conical spring; 4. Grain bar block; 5. Tension bolt; 6. Connecting shaft

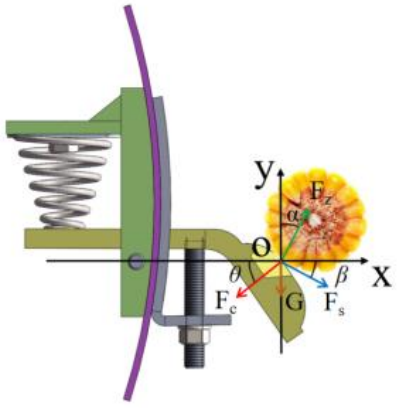

Fig. 3 - Analysis of the threshing force

Take a point of the corn cob impact threshing element, cross the connecting axis horizontal line direction at the point O to establish a coordinate OXY. When the threshing element is working, if the force F_c of the corn cob on the striker is sufficient to turn the striker block backward around the connecting axis as a circle, then the angle α and β will increase, and θ is constant. When the corn cob is in contact with the threshing element, the force in the direction of F_s is:

$$F_s = G\sin\beta - F_c\cos(\beta+\theta)\ [N] \quad (1)$$

Where: G is the gravity, N.

From the above equation (1), it can be obtained:

$$F_c = \frac{G\sin\beta - F_s}{\cos(\beta+\theta)}\ [N] \quad (2)$$

From the above equation, it can be seen that β increases the impact force F_c of the thresher on the cob. Then the threshing force on the cob also increases, which makes the corn cob easier to be threshed. At the same time, the conical spring under the threshing element is compressed, which acts as a cushion and reduces the impact of the thresher on the corn cob, which can reduce the broken rate of the corn kernels. Therefore, the conical spring as a flexible mechanism of the thresher work can greatly reduce the breaking of corn kernels when threshing.

Test Conditions and Instruments

In October 2021, the tests were carried out in the Agricultural Machinery Performance Laboratory of Shandong University of Science and Technology with the self-made variable stiffness threshing cylinder test bench. The test apparatus included a scraper-type cob lifter, an LDS-1G grain moisture meter (Ningbo Comet Instrument Co., Ltd.), a TESTO 465 digital tachometer (Detu Instruments International Trade Co., Ltd.), an ACS20 small electronic scale (Shanghai Huachao Electric Co., Ltd.), an 11kw three-phase asynchronous motor (Taizhou Yinniu Mechanical and Electrical Co., Ltd.) and a SAJ8000 series inverter (Guangzhou Sanjing Electric Co., Ltd.), etc. The test process is shown in Fig. 4.

Fig. 4 - Experimental process

The test material was selected from Zhengdan 958, and the basic characteristics of 50 corn ears were measured randomly using vernier calipers and LDS-1G grain moisture meter before the start of the test, and the values of the basic characteristics of corn ears are shown in Table 1.

Table 1

Corn parameters in experiment

Parameters	Value
Average ear length / mm	145.6
Average large end diameter / mm	50.2
Average small end diameter / mm	45.6
Kernel moisture content / %	27.6~28.5

Test Factors, Indicators and Methods

The corn threshing mechanism relies on the active rotation of the threshing element and the cob, the cob and the cob, the cob and the grating to generate force, ultimately achieving the threshing function *(Pužauskas et al., 2017).* Therefore, the threshing element and concave plate is the key components of the threshing device, its threshing element movement speed, concave clearance and feeding amount are the main factors affecting the threshing performance and kernel breakage.

After the experiment, the test results were measured in accordance with GB/T 21961-2008 "Test Methods for Corn Harvesting Machinery" and GB/T 21962-2020 "Corn Harvesting Machinery". At the end of each test, 2000 g of corn kernels were randomly selected from the kernel collection box, from which corn kernels with obvious cracks, damage, and broken skins were selected and weighed out to calculate the kernel breakage rate according to the following equation (3). During the measurement time, 2000 g of mixed kernels were taken from the kernel collection box, from which the mass of impurities was selected and weighed out to calculate the mass of mixed kernels and the impurity. The impurity rate was calculated according to equation (4).

Broken rate:

$$Z_s = \frac{m_s}{m_i} \times 100\ [\%] \quad (1)$$

Where: m_s is the mass of broken kernels sample, g; m_i is the mass of sample kernels; Z_s is the broken rate, %.

Impurity rate:

$$Z_z = \frac{m_{za}}{m_h} \times 100\ [\%] \quad (4)$$

Where m_{za} is the impurity quality, g; m_h is the mass of mixed grain, g; Z_z is the impurities rate, %.

RESULTS AND DISCUSSION

Orthogonal Test

Based on the results of the single-factor test, the regression analysis was performed on the data using Design-Expert 10.0.3 statistical software with cylinder speed (X_1), concave clearance (X_2) and feeding amount (X_3) as independent variables and the response values of the broken rate Y1 and impurity rate Y_2 of corn kernels, and the regression models of BR and IR were analyzed, and the experimental factor levels were arranged as shown in Table 2.

Table 2

Levels of parameters

Levels	Factors		
	Cylinder speed X_1 / ($r \cdot min^{-1}$)	Concave clearance X_2 / mm	Feed amount X_3 / ($kg \cdot s^{-1}$)
-1	350	35	6
0	400	40	7
1	450	45	8

Multi-factor Test Analysis

The test used the broken rate Y_1 and the impurity rate Y_2 as evaluation indices. Each test group was conducted three times in order to determine the mean value. The experimental design and outcomes are shown in Table 3.

Table 3

Results of multi-factorial tests

Test Number	X_1 ($r \cdot min^{-1}$)	X_2 (mm)	X_3 ($kg \cdot s^{-1}$)	BR (%)	IR (%)
1	-1	-1	0	3.75	6.25
2	1	-1	0	6.05	2.25
3	-1	1	0	2.15	5.07
4	1	1	0	4.75	4.11
5	-1	0	-1	2.16	4.05
6	1	0	-1	5.79	0.99
7	-1	0	1	3.01	4.02
8	1	0	1	6.13	2.15
9	0	-1	-1	3.82	0.83
10	0	1	-1	2.99	2.49
11	0	-1	1	4.45	2.59
12	0	1	1	3.88	3.15
13	0	0	0	3.21	1.33
14	0	0	0	2.86	1.05
15	0	0	0	2.34	1.86
16	0	0	0	2.66	1.15
17	0	0	0	2.88	1.52

The experimental data from Table 4 were subjected to an ANOVA with kernel broken rate and impurity rate as response values; the results are presented in Table 5.

The p value was used to determine the significance of the coefficients and also to test the interaction of the combined factors. As can be seen from the analysis in Table 4, for corn kernel broken rate, the model $p = 0.0005 < 0.001$, indicating that the fitted model reached a highly significant level; the out-of-fit term $p = 0.2129 > 0.05$, the out-of-fit term was not significant, indicating that the regression mathematical model fitted the actual results with high accuracy.

As can be seen from Table 4, ANOVA was performed on the kernel broken rate. the linear term of X_3 and the quadratic term of X_3 were both significant for the broken rate of kernels; the linear term of X_2 and the quadratic term of X_1 were both highly significant for the broken rate of kernels; and the linear term of X_1 was highly significant for the broken rate of kernels. Therefore, the order of the factors affecting the kernel broken rate was as follows: $X_1 > X_2 > X_3$. Since the smaller the broken rate of threshing, the better the quality of threshing.

Table 4

Analysis of variance for kernel broken rate

Variance Source	Sum of Squares of Deviations	Freedom *f*	*F* Value	*p*-Value	Significance Marker
Model	26.68	9	18.34	0.0005	***
X_1	16.97	1	104.96	< 0.0001	***
X_2	2.31	1	14.3	0.0069	**
X_3	0.92	1	5.68	0.0487	*
X_1X_2	0.023	1	0.14	0.7201	
X_1X_3	0.065	1	0.4	0.5461	
X_2X_3	0.017	1	0.1	0.7559	
X_1^2	3.69	1	22.83	0.002	**
X_2^2	0.85	1	5.25	0.0558	
X_3^2	1.26	1	7.77	0.027	*
Residual	1.13	7			
Lack of Fit	0.72	3	2.36	0.2129	not significant
Pure Error	0.41	4			
Cor Total	27.81	16			

Note: X_1 is cylinder speed / ($r \cdot min^{-1}$); X_2 is clearance between concave and cylinder/mm; X_3 is feed amount / ($kg \cdot s^{-1}$); * is significant ($p < 0.05$); ** is very significant ($p < 0.01$); *** is extremely significant ($p < 0.001$); *F* is Fischer's variance ratio; *p* is probability value.

As shown in Table 5, the impurity rate analysis was targeted and the linear terms of X_2 and X_3 and the quadratic terms of X_3 were significant for the impurity rate of the kernels; the interaction of X_1X_2 was highly significant for the impurity rate of the kernels; the linear terms of X1 and the quadratic terms of X_1 and X_2 were highly significant for the impurity rate of the kernels.

Table 5

Analysis of variance (ANOVA) for kernel impurity rate

Variance Source	Sum of Squares of Deviations	Freedom *f*	*F* Value	*p*-Value	Significance Marker
Model	39.07	9	33.08	< 0.0001	***
X_1	12.23	1	93.14	< 0.0001	***
X_2	1.05	1	8.01	0.0254	*
X_3	1.58	1	12	0.0105	*
X_1X_2	2.31	1	17.6	0.0041	**
X_1X_3	0.35	1	2.7	0.1445	
X_2X_3	0.3	1	2.3	0.1728	
X_1^2	13.46	1	102.52	< 0.0001	***
X_2^2	6.58	1	50.14	0.0002	***
X_3^2	0.57	1	4.33	0.0761	*

Variance Source	Sum of Squares of Deviations	Freedom *f*	*F* Value	*p*-Value	Significance Marker
Residual	0.92	7			
Lack of Fit	0.5	3	1.62	0.3179	not significant
Pure Error	0.41	4			
Cor Total	39.99	16			

Note: X_1 is cylinder speed/ (r·min^{-1}); X_2 is clearance between concave and cylinder/mm; X_3 is feed amount/ (kg·s^{-1}); * is significant ($p < 0.05$); ** is very significant ($p < 0.01$); *** is extremely significant ($p < 0.001$); *F* is Fischer's variance ratio; *p* is probability value.

Response Surface Analysis

To obtain the influence law of the experimental factors on each test index in a more intuitive manner, study the interaction effect of the other two factors by fixing one factor at zero levels, and transform the regression equation into a three-dimensional contour map using Design Expert10, as depicted in Fig. 5, Fig. 6 & Fig. 7.

$$BR = 1.79 + 1.48X_1 - 0.54X_2 + 0.32X_3 + 0.08X_1X_2 - 0.17X_1X_3 + 0.07X_2X_3 + 0.96X_1^2 + 0.43X_2^2 + 0.57X_3^2 \quad (5)$$

$$IR = 1.38 - 1.24X_1 + 0.36X_2 + 0.44X_3 + 0.76X_1X_2 + 0.29X_1X_3 - 0.27X_2X_3 + 1.79X_1^2 + 1.25X_2^2 - 0.37X_3^2 \quad (6)$$

From Fig. 5(a), it can be seen that when the concave clearance is 40 mm. At a particular cylinder speed, the kernel broken rate falls and then increases as the feeding amount increases. When the feeding amount increases to approximately 7 kg/s, as depicted in figure 5a, the threshing mode changes from striking to rubbing and threshing of corn, which decreases the breaking rate due to an increase in the amount of corn cob in the concave clearance.

As shown in Fig. 5(b), the impurity rate of kernels increased and then decreased with the increase of feeding amount. When the feeding amount is low, the spike tooth inside the cylinder has less impact on the cob and the mutual rubbing effect between the cob and the cob is weak, which is not conducive to the separation of the kernels and the cob, so the impurity rate is larger.

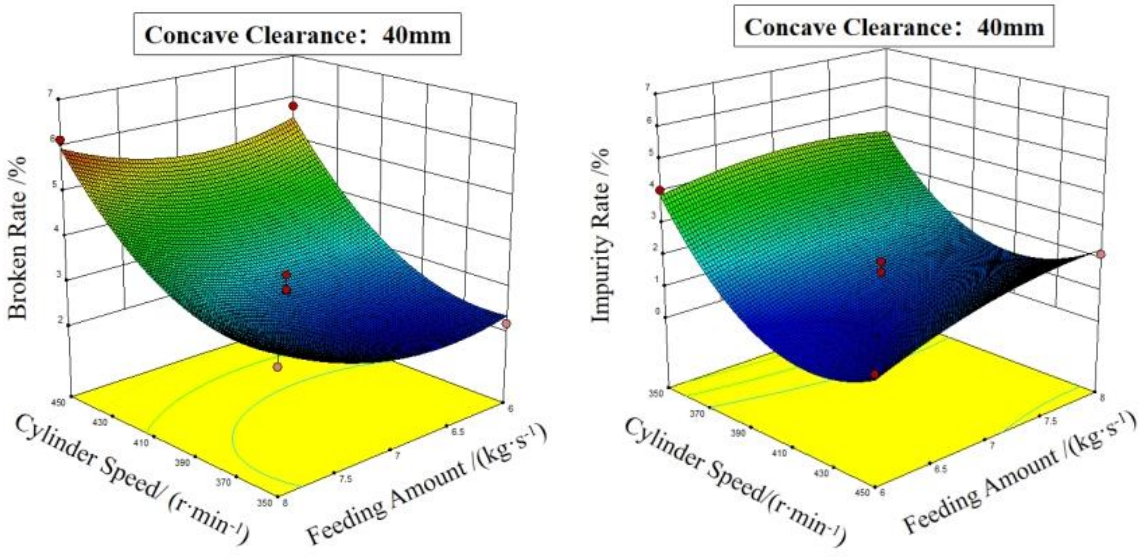

(a) (b)

Fig. 5 - Response surface diagrams of interaction

(a) Interaction of the cylinder speed and feeding amount on broken rate;
(b) Interaction of the cylinder speed and feeding amount on the impurity rate.

From Fig. 6(a), it can be seen that the increase of concave clearance leads to a slight decrease and then an increase of kernel broken first. It may be because when the feeding amount is small, the threshing space is relatively sufficient, and the change of the concave clearance has less influence on the degree of material filling. From Fig. 6(b), it can be seen that the first reduction in impurity rate gradually increases with the increase in the concave clearance. This is because as the concave clearance increases, the influence of the threshing element on the cob diminishes and the mutual squeezing and friction effects between the cobs diminish, leading to an increase in the impurity rate.

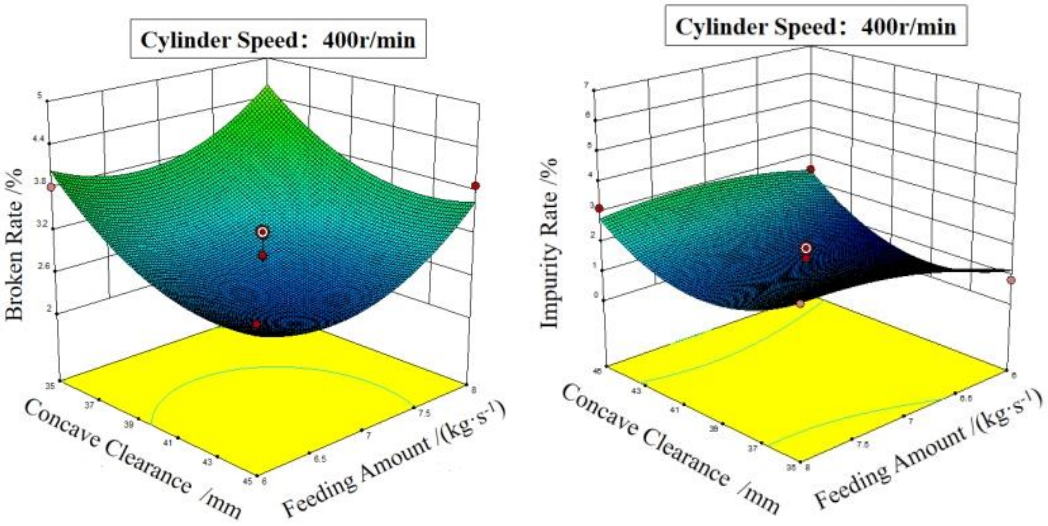

(a) (b)

Fig. 6 - Response surface diagrams of interaction

(a) Interaction of the concave clearance and feeding amount on broken rate;
(b) Interaction of the concave clearance and feeding amount on the impurity rate.

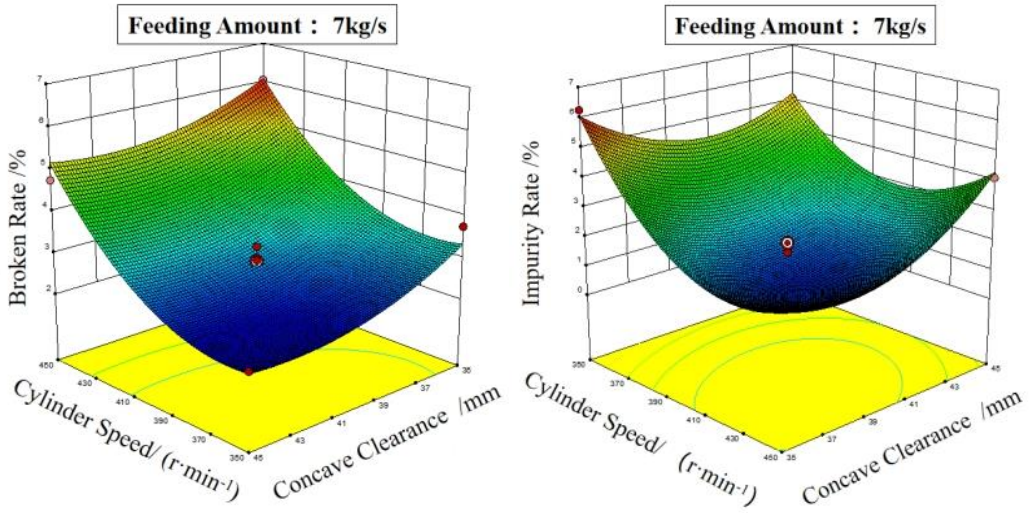

(a) (b)

Fig. 7 - Response surface diagrams of interaction

(a) Interaction of the cylinder speed and concave clearance on broken rate;
(b) Interaction of the cylinder speed and concave clearance on the impurity rate.

From Fig. 7(a), it can be seen that as the cylinder speed increases, the kernel broken rate increases; and as the concave clearance increases, the kernel broken rate shows a decreasing trend. When the cylinder speed increased, the linear velocity of the spike teeth striking the corn increased, which then led to an increase in the collision velocity and a higher broken rate. When the concave clearance increased, the broken rate decreases because the crushing effect of the nail tooth and the concave clearance on the corn cob is reduced.

Fig. 7(b) shows that as the cylinder speed increases, the impurity rate decreases, and as the gap between the concave plate's increases, the impurity rate increases. When the cylinder speed increases, the impact of the spike tooth on the corn cob is enhanced, and the corn kernels are more easily dislodged from the cob, so the impurity rate decreases. When the concave clearance increases, the extrusion of the threshing cylinder to the corn cob and the kneading effect between the corn and the corn are weakened, and the kernels are not easy to come off from the cob, so the rate of impurity increases.

Verification Experiment

The regression equation was solved by Design-Expert software and the optimal operating parameters (decimals rounded) for the results averaged over the variable stiffness corn flexible threshing device was: cylinder speed 392 r·min^{-1}, concave clearance 40 mm, and feeding rate 6.1 kg·s^{-1}. Under these conditions: broken rate 1.67 % and impurity rate 1.03 %.

$$\begin{cases} \mathrm{BR} = \text{minimize} \\ \mathrm{IR} = \text{minimize} \\ 350 < \mathrm{X}_1 < 450 \\ 35 < \mathrm{X}_2 < 45 \\ 6 < \mathrm{X}_3 < 8 \end{cases} \quad (7)$$

To verify the reliability of the regression model, the results were averaged over three trials of the above optimal threshing operation parameters, and the test results showed that the mean value of the broken rate was 1.74% and the mean value of the impurity rate was 0.98%. The relative error with the predicted value is less than 5%, which indicates that the accuracy of the regression model is high. The test results still meet the requirements of the national standard.

CONCLUSIONS

(1) The variable stiffness corn threshing element is designed to reduce the impact on the corn kernels, which can reduce the kernel broken rate.

(2) The optimum values of the operating parameters of the corn threshing unit were determined by multi-factor tests. The ANOVA of the test results showed that the cylinder speed was 392 r·min^{-1}, the concave clearance was 40 mm, and the feed amount was 6.1 kg·s^{-1}. The BR was 1.47% and the IR was 1.03%.

(3) Threshing cylinder speed, concave clearance and feeding amount had significant effects on corn kernel broken rate and impurity rate.

Currently, only one variety of corn has been tested in this study. The team will continue to test different varieties of corn in the field to further validate the threshing performance and adaptability of the designed threshing device.

ACKNOWLEDGEMENT

This research was funded by the National Key R&D Program of China, grant number 2021YFD2000502, the Natural Science Foundation of Shandong Province, grant number ZR202111290044.

REFERENCES

[1] Akubuo, C. O. (2002). PH—Pastharvest Technology: Performance Evaluation of a Local Maize Sheller. *Biosystems Engineering*, Vol. 83, 77-83. England. https://doi.org/10.1006/bioe.2002.0095

[2] Bratan, S., Safonov, V., Zhalnin, E., Lapa, M., & Bordan, D. (2019). Use of vortex flows for aerodynamic threshing of agricultural crops. *E3S Web of Conferences*, Vol. 126. Russia. https://doi.org/10.1051/e3sconf/201912600004

[3] Chai, X., Zhou, Y., Xu, L., Li, Y., Li, Y., & Lv, L. (2020). Effect of guide strips on the distribution of threshed outputs and cleaning losses for a tangential-longitudinal flow rice combine harvester. *Biosystems Engineering*, Vol. 198, 223-234. England. https://doi.org/10.1016/j.biosystemseng.2020.08.009

[4] Chen, Z., Wassgren, C., & Ambrose, K. (2020). A Review of Grain Kernel Damage: Mechanisms, Modeling, and Testing Procedures. *Transactions of the ASABE*, 63(2), 455-475. https://doi.org/10.13031/trans.13643

[5] Feng, J., Wu, Z., Qi, D., Jin, Y., & Wu, W. (2019). Accurate measurements and establishment of a model of the mechanical properties of dried corn kernels. *International Agrophysics*, Vol. 33, 373-381. Poland. https://doi.org/10.31545/intagr/110845

[6] Fu, Q., Fu, J., Chen, Z., Han, L., & Ren, L. (2019). Effect of impact parameters and moisture content on kernel loss during corn snapping. *International Agrophysics*, Vol. 33, 493-502. Poland. https://doi.org/10.31545/intagr/113490

[7] Kiniulis, V., SteponaviČIus, D., KemzŪRaitĖ, A., AndriuŠIs, A., JukneviČIus, D. (2018). Dynamic Indicators of a Corn Ear Threshing Process Influenced by the Threshing-Separation Unit Load. *Mechanics*, Vol. 24, 412-421. Lithuania. https://doi.org/10.5755/j01.mech.4.24.20721

[8] Li, X., Du, Y., Guo, J., Mao, E. (2020). Design, Simulation, and Test of a New Threshing Cylinder for High Moisture Content Corn. *Applied Sciences*, Vol. 10, 4925. Switzerland. https://doi.org/10.3390/app10144925

[9] Pakhomov, V. I., Braginets, S. V., Bakhchevnikov, O. N., Benova, E. V., Rukhlyada, A. I. (2020). Experimental Data of the Ear Threshing Process in a Pneumatic Device. *Engineering Technologies and Systems*, Vol. 30, 111-132. Russian Federation. https://doi.org/10.15507/2658-4123.030.202001.111-132

[10] Pužauskas, E., Steponavičius, D., Jotautienė, E., Petkevičius, S., & Kemzūraitė, A. (2017). Substantiation of concave crossbar shape for corn ear threshing. *Mechanics*, 22(6). https://doi.org/10.5755/j01.mech.22.6.16370

[11] Wang, B., Wang, J. (2019). Mechanical properties of maize kernel horny endosperm, floury endosperm and germ. *International Journal of Food Properties*, Vol. 22, 863-877. United States. https://doi.org/10.1080/10942912.2019.1614050

[12] Wang, D., Tian, H., Zhang, T., He, C., & Liu, F. (2021). Dem Simulation and Experiment of Corn Grain Grinding Process. *Engenharia Agricola*, 41(5), 559-566. https://doi.org/10.1590/1809-4430-eng.agric.v41n5p559-566/2021

[13] Shahbazi, F., Shahbazi, R. (2018). Mechanical Damage to Corn Seeds. *Cercetari Agronomice in Moldova*, Vol. 51, 1-12. Poland. https://doi.org/10.2478/cerce-2018-0021

[14] Srison, W., Chuan-Udom, S., Saengprachatanarak, K. (2016). Effects of operating factors for an axial-flow corn shelling unit on losses and power consumption. *Agriculture and Natural Resources*, Vol. 50, 421-425. Thailand. https://doi.org/10.1016/j.anres.2016.05.002

[15] Su, Z., Li, Y., Dong, Y., Tang, Z., Liang, Z. (2020). Simulation of rice threshing performance with concentric and non-concentric threshing gaps. *Biosystems Engineering*, Vol. 197, 270-284. England. https://doi.org/10.1016/j.biosystemseng.2020.05.020

[16] Xie, F., Luo, X., Lu, X., Sun, S., Tang, C. (2009). Experiment on the influence of flexible drum structure parameters on rice threshing effect (柔性滚筒结构参数对水稻脱粒效果的影响试验). *Research on Agricultural Mechanization*, Vol. 31, 147-151. Heilongjiang/China.

[17] Yang, R., Chen, D., Zha, X., Pan, Z., Shang, S. (2021). Optimization Design and Experiment of Ear-Picking and Threshing Devices of Corn Plot Kernel Harvester. *Agriculture*, Vol. 11, 904. Switzerland. https://doi.org/10.3390/agriculture11090904

[18] Yang, H., Cao, M., Wang, B., Hu, Z., Xu, H., Wang, S., Yu, Z. (2022). Design and Test of a Tangential-Axial Flow Picking Device for Peanut Combine Harvesting. *Agriculture*, Vol. 12, 179. Switzerland. https://doi.org/10.3390/agriculture12020179